

Three-dimensional graphitic carbon sphere foams as sorbents for cleaning oil spills

Saisai Li, Haijun Zhang, Longhao Dong, Haipeng Liu, and Quanli Jia

Cite this article as:

Saisai Li, Haijun Zhang, Longhao Dong, Haipeng Liu, and Quanli Jia, Three-dimensional graphitic carbon sphere foams as sorbents for cleaning oil spills, *Int. J. Miner. Metall. Mater.*, 29(2022), No. 3, pp. 513-520. <https://doi.org/10.1007/s12613-020-2180-3>

View the article online at [SpringerLink](#) or [IJMMM Webpage](#).

Articles you may be interested in

Wen-zhan Huang, Hong-jie Luo, Yong-liang Mu, Hao Lin, and Hao Du, [Low-frequency damping behavior of closed-cell Mg alloy foams reinforced with SiC particles](#), *Int. J. Miner. Metall. Mater.*, 24(2017), No. 6, pp. 701-707. <https://doi.org/10.1007/s12613-017-1453-y>

Qi Wang, Yue-yong Du, Yan-qing Lai, Fang-yang Liu, Liang-xing Jiang, and Ming Jia, [Three-dimensional antimony sulfide anode with carbon nanotube interphase modified for lithium-ion batteries](#), *Int. J. Miner. Metall. Mater.*, 28(2021), No. 10, pp. 1629-1635. <https://doi.org/10.1007/s12613-021-2249-7>

Dan Wang, Qun Ma, Kang-hui Tian, Chan-Qin Duan, Zhi-yuan Wang, and Yan-guo Liu, [Ultrafine nano-scale Cu₂Sb alloy confined in three-dimensional porous carbon as an anode for sodium-ion and potassium-ion batteries](#), *Int. J. Miner. Metall. Mater.*, 28(2021), No. 10, pp. 1666-1674. <https://doi.org/10.1007/s12613-021-2286-2>

Min-nan Feng, Yu-cong Wang, Hao Wang, Guo-quan Liu, and Wei-hua Xue, [Reconstruction of three-dimensional grain structure in polycrystalline iron via an interactive segmentation method](#), *Int. J. Miner. Metall. Mater.*, 24(2017), No. 3, pp. 257-263. <https://doi.org/10.1007/s12613-017-1403-8>

Huan-yu Zhang, Rui Li, Wen-wu Liu, Mei Zhang, and Min Guo, [Research progress in lead-less or lead-free three-dimensional perovskite absorber materials for solar cells](#), *Int. J. Miner. Metall. Mater.*, 26(2019), No. 4, pp. 387-403. <https://doi.org/10.1007/s12613-019-1748-2>

Xue-feng Bai, Yan-hui Sun, Rui-mei Chen, Yi-min Zhang, and Yi-fan Cai, [Formation and thermodynamics of CaS-bearing inclusions during Ca treatment in oil casting steels](#), *Int. J. Miner. Metall. Mater.*, 26(2019), No. 5, pp. 573-587. <https://doi.org/10.1007/s12613-019-1766-0>



IJMMM WeChat



QQ author group

Three-dimensional graphitic carbon sphere foams as sorbents for cleaning oil spills

Saisai Li^{1,2}, Haijun Zhang²,, Longhao Dong², Haipeng Liu², and Quanli Jia³

1) Key Laboratory of Green Fabrication and Surface Technology of Advanced Metal Materials, Anhui University of Technology, Ma'anshan 243002, China

2) The State Key Laboratory of Refractories and Metallurgy, Wuhan University of Science and Technology, Wuhan 430081, China

3) High Temperature Ceramic Institute, Zhengzhou University, Zhengzhou 450052, China

(Received: 22 May 2020; revised: 22 August 2020; accepted: 26 August 2020)

Abstract: Frequent offshore oil spill accidents, industrial oily sewage, and the indiscriminate disposal of urban oily sewage have caused serious impacts on the human living environment and health. The traditional oil–water separation methods not only cause easily environmental secondary pollution but also a waste of limited resources. Therefore, in this work, three-dimensional (3D) graphitic carbon sphere (GCS) foams (collectively referred hereafter as 3D foams) with a 3D porous structure, pore size distribution of 25–200 μm , and high porosity of 62vol% were prepared for oil adsorption via gel casting using GCS as the starting materials. The results indicate that the water contact angle (WCA) of the as-prepared 3D foams is 130°. The contents of GCS greatly influenced the hydrophobicity, WCA, and microstructure of the as-prepared samples. The adsorption capacities of the as-prepared 3D foams for paraffin oil, vegetable oil, and vacuum pump oil were approximately 12–15 g/g, which were 10 times that of GCS powder. The as-prepared foams are desirable characteristics of a good sorbent and could be widely used in oil spill accidents.

Keywords: graphitic carbon spheres; three dimensional; foams; gel casting; oil adsorption

1. Introduction

In recent years, oil spill accidents have frequently happened during extraction, transportation, transfer, and storage processes, leading to high risks and frequencies of oil leakages, which seriously polluted the marine environment [1–2]. Oil leakages in the natural environment not only cause a great loss of energy but also have catastrophic effects on the environment and ecosystem [3]. Several techniques have been developed to solve the oil leakage problem, such as mechanical extraction [4], *in situ* burning [5], chemical modification [6], biological oxidation [7], and physical adsorption methods [8]. The first four methods have limitations, such as secondary pollution, high cost, and complex operation [9]. The last one, i.e., physical adsorption methods, is considered the most efficient technique for the treatment of oil spills because of its easy operation, friendly environment, and low energy consumption [10]. Zeolites [11], kaolinite [12], goethite [13], and Si-MCM-41 [14] are commonly used as adsorbents, but these adsorbents have shortcomings, such as low adsorption capacity and tedious recovery process [15]. Therefore, the development of highly effective adsorbent materials is of primary importance for the removal of oil spillage and chemical leakage in the environment [16].

Currently, three-dimensional (3D) porous materials with

hydrophobic and oleophilic properties are becoming the most popular materials that can be used for oil adsorption because of their high porosity and high adsorption capacities [16–18]. Up to now, most published studies have been focused on polyurethane foam [19], wax modified plants [20], and melamine sponge-based 3D porous materials [21], which suffer from complex preparation processes and large waste volumes. Moreover, the template method is most commonly used for many 3D porous materials, but it also has a relatively complex template removal process and wastes template materials, such as SiO_2 and zeolite. In comparison, the gel casting foaming technique combined with freeze drying has easy operation and is environment friendly.

Recently, carbon materials, such as graphene, activated carbon, carbon nanotube, and graphitic carbon spheres (GCS) [22–33], have attracted much attention. Among which, GCS are becoming a more valuable alternative for preparing 3D porous foams applied in oil leakages owing to their high specific surface area, good dispersion, great liquidity, and hydrophobicity. Hence, in this work, 3D GCS foams (collectively referred hereafter as 3D foams) were synthesized via gel casting combined with freeze drying using GCS as carbon sources, sodium lauryl sulfate (SDS) as the foaming agent, gelatin as the crosslinking agent, and stearic acid and epoxy resin as the foam stabilizer and binder agents. The

 Corresponding author: Haijun Zhang E-mail: zhanghaijun@wust.edu.cn

© University of Science and Technology Beijing 2022

effects of the amounts of GCS, gelatin, and resin on the preparation of 3D foams were studied. Moreover, the adsorption capacities of as-prepared 3D foams for different kinds of oils were examined.

2. Experimental

2.1. Raw materials

The main materials used in this study are SDS, gelatin, stearic acid, epoxy resin, and deionized (DI) water. The SDS, gelatin, and stearic acid were obtained from Sinopharm Chemical Reagent Co., Ltd. (Shanghai, China), and the epoxy resin was obtained from Kunshan Ivdun Chemical Co., Ltd. (Jiangsu, China). All chemicals used were of analytical grade and were used as received without any further purification.

2.2. Preparation of 3D foams

The GCS were first prepared according to the method introduced in our previous article [33]. Then, the SDS, gelatin, stearic acid, epoxy resin, and GCS were mixed in DI water at a fixed mass ratio with strong stirring to produce a foam slurry, and the mixture was directly subjected to freezing to form foam monoliths. Finally, the 3D foams were prepared after heat treatment at 110°C for 24 h.

2.3. Characterization

A powder X-ray diffraction (XRD) analysis using a Philips X'Pert PRO diffractometer (X'Pert PRO, Philips, Hillsboro, The Netherlands) equipped with a Cu K α radiation ($\lambda = 0.1542$ nm) was employed to examine the as-prepared sample at 40 mA and 40 kV. The microstructures and morphologies of the final products were observed using a field-emission scanning electron microscope (FE-SEM, Nova 400 nanoSEM, FEI, USA). Water wettability of the samples was evaluated by measuring the water contact angle (WCA) using an optical contact angle measuring system with a high-speed USB camera angle (WCA) and a video-bra (Dataphysics OCA15Pro). Then, the pore size distribution was measured using mercury intrusion porosimetry (Quantachrome PM60GT-18, Quantachrome Instruments Ltd., USA). Nitrogen adsorption/desorption measurements were performed using a gas sorption analyzer (Autosorb-1-MP/LP, Quantachrome, USA). The samples were out-gassed at 150°C for 3 h under vacuum in the degas port, and the specific surface area was calculated using the Brunauer–Emmett–Teller model.

2.4. Adsorption experiments

The absorption capacities of the as-prepared GCS and 3D foams were determined by a weight measurement with three different kinds of oils. For the GCS powder, the measured procedure was as follows: the mass of the GCS was first determined, and the adsorbed oil on the GCS was dropped. The GCS reached their maximum adsorption capacity after they were completely wetted by oil, and then the added mass was regarded as the weight of the adsorbed oil. For the as-prepared 3D foams, the foam was taken in and weighed first, re-

ording it as W_0 , and then immersed in the oil liquid for 10 min. Then, the foam was taken out, and the sample filled with oil liquid was weighed, recording it as W_1 . Each sample was performed thrice, and the average values were taken as the adsorption capacity (Q) of the sample. Q is calculated according to the following formula:

$$Q = \left(\frac{W_1}{W_0} - 1 \right) \quad (1)$$

3. Results and discussion

3.1. Adsorption properties of GCS for oil pollutants

The GCS possess a high specific surface area of approximately 564 m²/g, good dispersion, great liquidity, and hydrophobicity properties. They were prepared via hydrothermal carbonization combined with the catalytic graphitization method using glucose as carbon sources; these methods have low cost of raw materials and a simple preparation process [33]. To investigate the hydrophobicity and lipophilicity of the prepared GCS, the wetting property of pressed GCS with a dimension of 20 mm (diameter) \times 5 mm (height) was tested by the WCA. Fig. 1 shows that the GCS have a hydrophobic surface with a WCA of approximately 133°, which might be attributed to the high graphitization degree of the CGS (Fig. 2(a)). As shown in Fig. 2(a), the GCS exhibited an evident peak at 26.3°, which was assigned to the characteristic {002} plane of graphite (ICDD 01-075-1621), indicating the presence of graphitic carbon in the GCS. Moreover, the GCS adsorption capacities were approximately 1.0–1.5 times of their own weights and increased with the increase in oil densities for paraffin oil, vegetable oil, and vacuum pump oil (Fig. 2(b)).

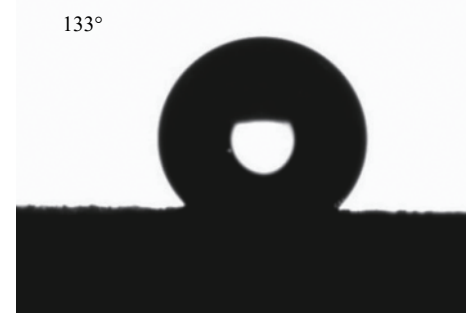


Fig. 1. Water contact angle of the as-prepared pressed graphitic carbon sphere.

3.2. Adsorption properties of 3D foams for oil pollutants

3.2.1. Effect of GCS addition on the preparation of the 3D foams for oil adsorption

Fig. 2(b) shows that the adsorption capacity of GCS to oil pollutants is limited. To further enhance the adsorption capacity, the 3D foams were prepared using GCS as the carbon source. As shown in Fig. 3, the water droplets with a spherical shape can be stable for a long time on the foam, indicating

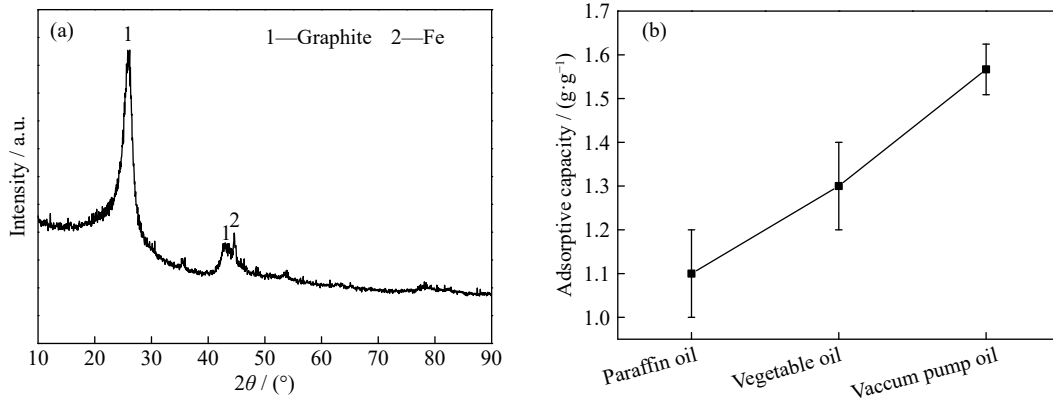


Fig. 2. X-ray diffraction pattern (a) and adsorption capacities (b) of the as-prepared graphitic carbon sphere for paraffin oil, vegetable oil, and vacuum pump oil.

the hydrophobicity nature of the as-prepared foam. The WCAs of the foams with different amounts of GCS are shown in Fig. 4 (fixed SDS content = 1.7wt%, gelatin content = 4.2wt%, and resin content = 8.3wt%). The WCA was approximately 130° for the sample without any GCS. With the GCS amount increased to 0.42wt%, the WCA decreased to approximately 120° , and the water droplets gradually immersed in the foam. The phenomenon might be attributed to the change in the morphology and pore structure of the as-prepared foams after adding the GCS. By further increasing the GCS by 0.83wt%–1.65wt%, the WCAs increased to approximately 130° again because of the hydrophobicity property of the GCS. XRD was investigated to confirm the structure of the as-prepared 3D foam prepared with 0.83wt% GCS (fixed SDS content = 1.7wt%, gelatin content = 4.2wt%, and resin content = 8.3wt%). The peak corresponded to the $\{002\}$ plane of the graphite still existing in the sample (Fig. 5). However, its crystallinity was lower than that of GCS (Fig. 2(a)), which might be attributed to the amorphous carbon brought about by the added organic materials (gelatin and resin) during the foaming process. The XRD results again confirmed that adding GCS during the foaming process increased the hydrophobicity property of the foams (Fig. 5).

Fig. 6 shows the SEM images of the specimens whose WACs are shown in Fig. 4, clearly demonstrating the effects of GCS amounts on the morphology of the 3D foams. Without GCS, the foams were mainly composed of window pores with a pore size distribution of approximately 50–100 μm (Fig. 6(a)). When GCS was added into the foams, the morphology of the as-prepared sample exhibited a 3D irregular network structure (Fig. 6(b–e)), which may be attributed to the defoaming phenomenon resulting from the addition of



Fig. 3. Macroscopic digital photographs of water droplets on the graphitic carbon sphere foam.

GCS during the preparation process.

The porosity and pore size distributions of the 3D foams were characterized by mercury intrusion porosimetry and shown in Fig. 7. With the increasing contents of GCS, the porosity of the foam gradually increased first and then decreased (Fig. 7(a)), and the pore size distributions also became wider and concentrated in the range of 25–200 μm with the added GCS amounting to 0.42wt%–1.65wt%. This result indicates that the addition of GCS destroyed the pore structure and widened the pore size distributions of the samples (Fig. 7(b)), which agrees well with the SEM results presented in Fig. 6.

Finally, the adsorption properties of the as-prepared 3D foams were examined. As shown in Fig. 8, the adsorption capacities for the oil of the foams was much higher than that of the original GCS. With the increase in GCS dosages, the adsorption capacities of the 3D foams initially increased and

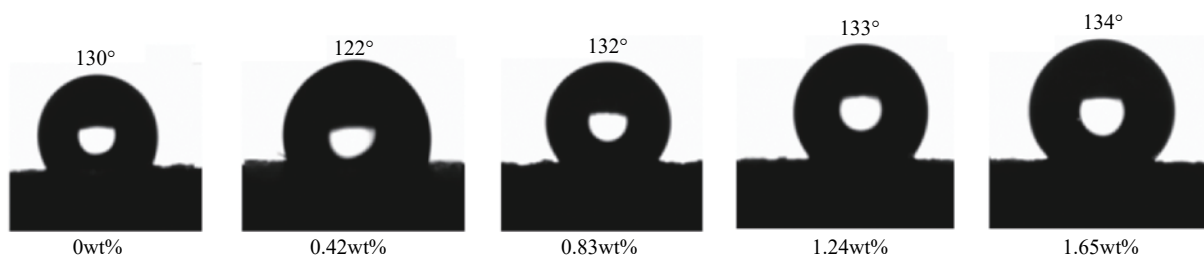


Fig. 4. Water contact angles of the 3D foams with different amounts of graphitic carbon spheres.

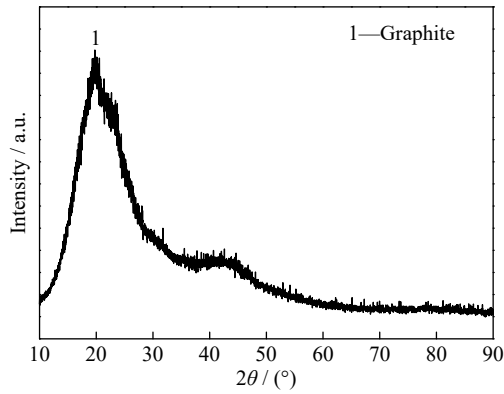


Fig. 5. X-ray diffraction pattern of the as-prepared 3D foam with 0.83wt% graphitic carbon spheres (fixed SDS content = 1.7wt%, gelatin content = 4.2wt%, and resin content = 8.3wt%).

then decreased again, and the optimal GCS content was 0.83wt%, which were consistent with the porosity and pore size distributions of the samples (Fig. 7). To investigate the

effect of the specific surface area of the as-prepared 3D foams on the oil adsorption, the specific surface areas of the 3D foams without GCS and with 0.83wt% GCS (fixed SDS content = 1.7wt%, gelatin content = 4.2wt%, and resin content = 8.3wt%) were evaluated using N_2 adsorption and desorption (Fig. 9), which were $0.24 \text{ m}^2/\text{g}$ and $0.33 \text{ m}^2/\text{g}$, respectively. Both of them were much lower than that of GCS ($564 \text{ m}^2/\text{g}$) [33]. The higher oil adsorption capacity of the as-prepared foams, compared with that of GCS, indicated that the oil adsorption performance mainly depended on macropores in the as-prepared samples.

3.2.2. Effect of gelatin addition on the preparation of 3D foams for oil adsorption

Gelatin as a crosslinking agent has a great influence on the pore size distributions and mechanical strengths of the foams. The addition of gelatin on the preparation of 3D foams was examined, and the findings are shown in Figs. 10–11. The findings demonstrated that the WCAs presented an increasing trend with increasing gelatin amounts, which might be at-

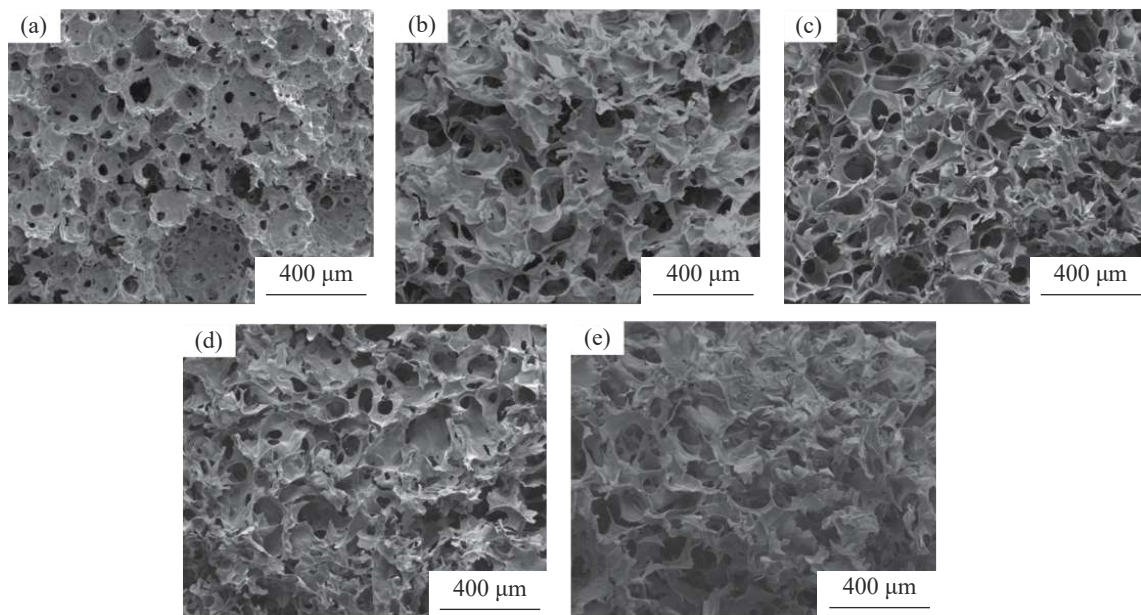


Fig. 6. Scanning electron microscopy images of the 3D foams prepared with different amounts of graphitic carbon spheres: (a) 0wt%; (b) 0.42wt%; (c) 0.83wt%; (d) 1.24wt%; (e) 1.65wt%.

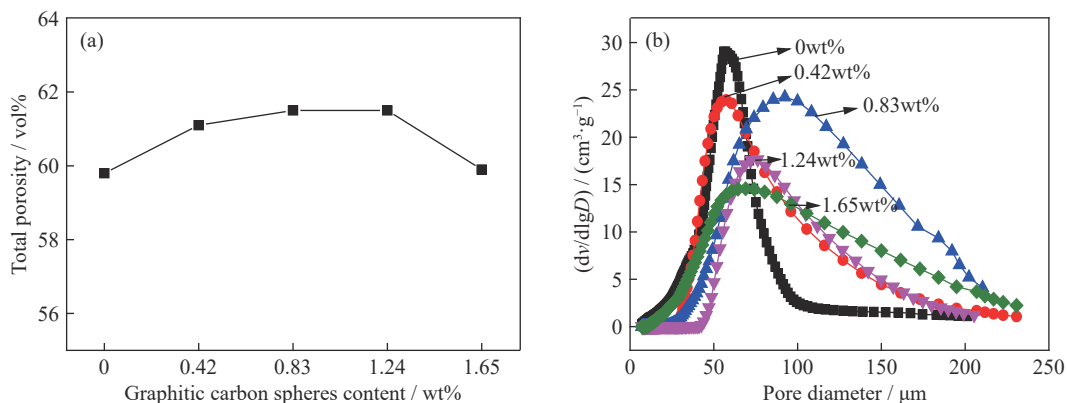


Fig. 7. Total porosity (a) and pore size distributions (b) of the 3D foams prepared with different amounts of graphitic carbon spheres.

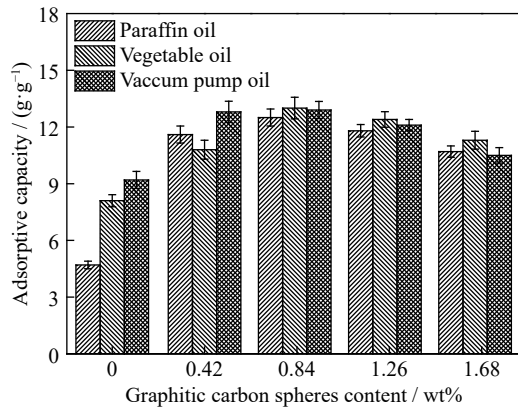


Fig. 8. Adsorption capacities of 3D foams with different oils.

tributed to the increase in the viscosity of the solution and the decrease in the total porosity and pore size distribution of the foam (Fig. 11). The WCAs of the as-prepared 3D foams accordingly increased with the decrease in the pore size of the foams, which might be attributed to the increase in the water contacted areas, defects, and roughness, and finally, the WCAs were enhanced [34]. Moreover, the morphologies of the samples were similar with the SEM results presented above (Fig. 6(b–e)).

The porosity and pore size distributions of the as-prepared 3D foams were characterized by mercury intrusion porosimetry, as shown in Fig. 11. The porosity of the foams decreased with the increase in the gelatin content (Fig. 11(a)), and the pore size distributions gradually narrowed (Fig. 11(b)), which might be ascribed to the increase in the viscosity of the initial gel solution as the gelatin amounts increased, leading to decreased porosity.

The oil adsorption capacities of the as-prepared 3D foams

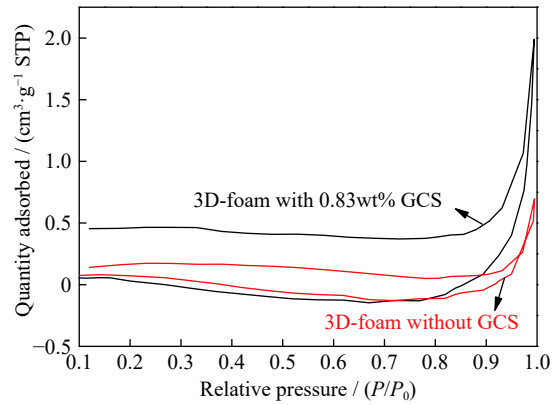


Fig. 9. N₂ adsorption–desorption isotherm of 3D foams with 0.83wt% GCS (fixed SDS content = 1.7wt%, gelatin content = 4.2wt%, resin content = 8.3wt%).

with different gelatin contents showed that when the gelatin amounts increased from 2.6wt% to 4.2wt%, the adsorption capacities were quite similar. However, when the gelatin content was further increased to (5.0–5.8)wt%, the adsorption capacities of the samples decreased (Fig. 12). The main reason can be attributed to the decrease in the foam porosities (Fig. 11(a)). In a word, the optimal addition of gelatin was 4.2wt%.

3.2.3. Effect of resin addition on the preparation of 3D foams for oil adsorption

In addition, by fixing the GCS, gelatin, and foaming agent amounts to 0.83wt%, 4.2wt%, and 1.7wt%, respectively, the effect of resin addition on the adsorption capacities of the 3D foams was also studied. The WCAs of the foams with different resin amounts were approximately 130° (Fig. 13), and the morphologies of the samples were all 3D network structures

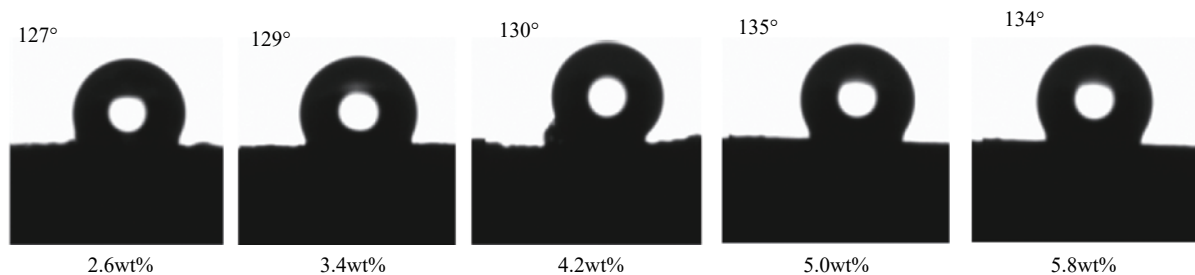


Fig. 10. Water contact angles of graphitic carbon sphere foam prepared with different contents of gelatin.

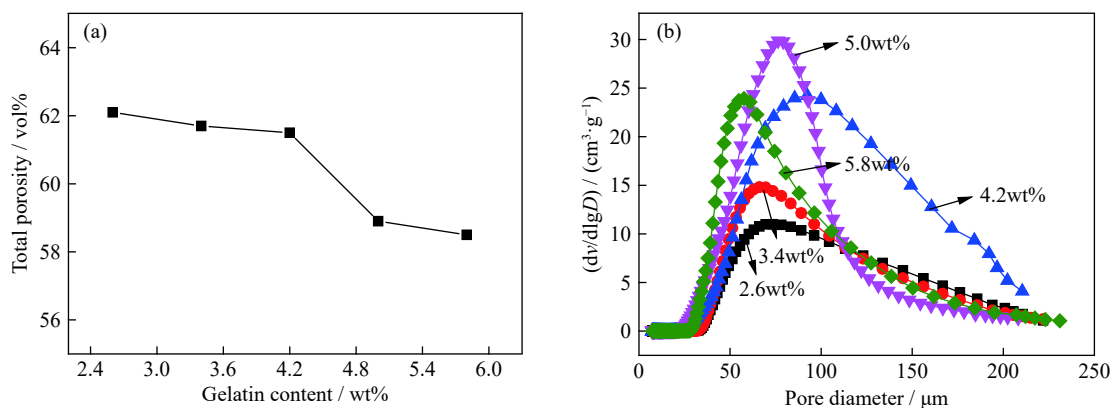


Fig. 11. Total porosity (a) and pore size distributions (b) of the 3D foams prepared with different amounts of gelatin.

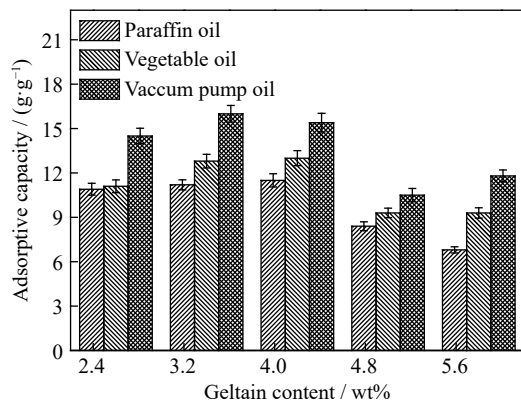


Fig. 12. Adsorption capacities of 3D foams with different amounts of gelatin.

with the interconnected pores ranging from tens to hundreds of micrometers, as shown in the above results. However, the porosities of the foams gradually decreased with the increas-

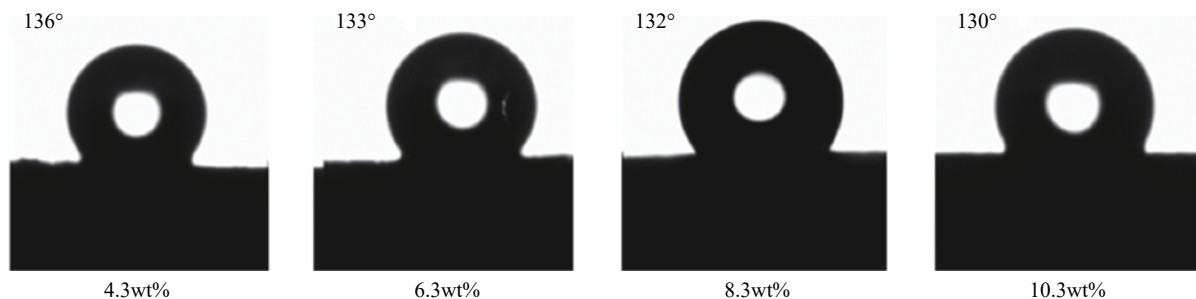


Fig. 13. Water contact angles of the 3D foams prepared with different contents of resin.

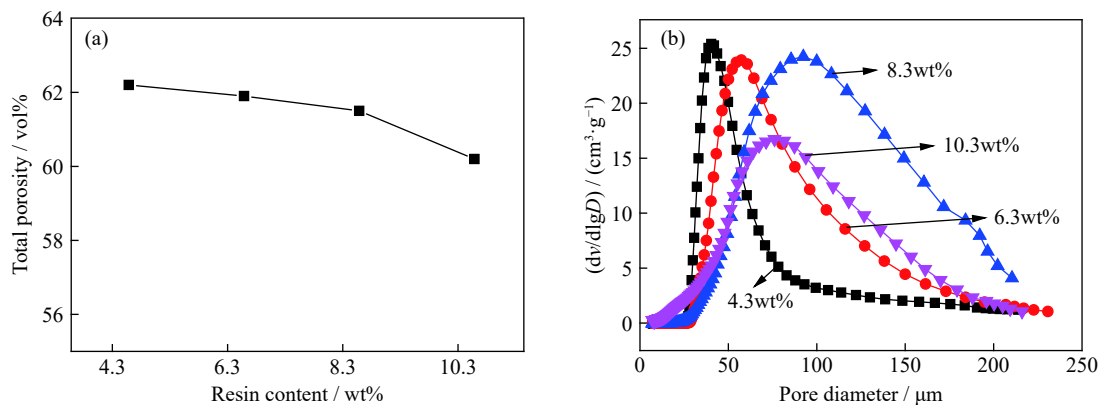


Fig. 14. Total porosity (a) and pore size distributions (b) of the 3D foams prepared with different amounts of resin.

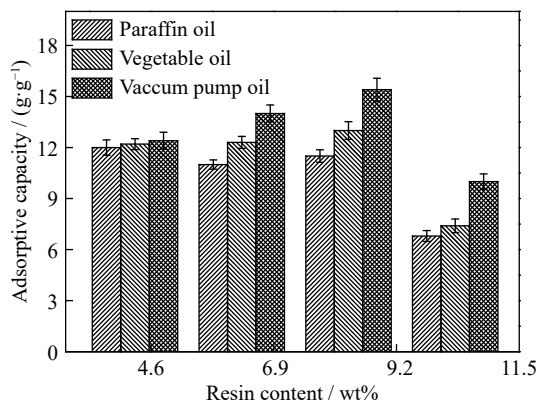


Fig. 15. Adsorption capacities of as-prepared 3D foams prepared with different amounts of resin.

ing resin amounts (Fig. 14(a)), and the pore size distributions first increased and then decreased (Fig. 14(b)). Based on the above-mentioned results, the optimal resin amount is 8.3wt%. A proper amount of resin was in favor of the foaming process, and the viscosity of the gel solution will increase due to the introduction of high amounts of resin and weaken the foaming process. These effects may result in the initial increase in the pore size distributions of the samples and then decrease with the increasing resin amounts.

Fig. 15 shows the adsorption capacities of as-prepared 3D foams by adding different amounts of resin. The total adsorption capacities of the samples first increased and then slightly decreased, which were consistent with the porosity results shown in Fig. 14. Thus, under the experimental conditions, the optimal preparation conditions for the 3D foams are 0.83wt% for GCS, 4.2wt% for gelatin, and 8.3wt% for resin.

4. Conclusion

In view of the present oil spill accidents, materials with high porosity and hydrophobicity properties are becoming important materials that can be used in oil adsorption. In this work, a simple and feasible foam gel casting method was successfully developed to prepare 3D GCS foams for oil adsorption. The as-prepared 3D foams possessed a high porosity of 62vol% with a pore size distribution of 25–200 μm, and a 3D porous structure. Moreover, the amounts of GCS had a great influence on the hydrophobicity, WCAs, and microstructure of the as-prepared 3D foams. The WCA of the as-prepared foam was approximately 130°, and the adsorption capacities for oil were approximately 12–15 g/g, which were

10 times those of starting GCS powders, indicating that the as-prepared 3D foams have a potential application prospect in oil spill pollution. The present work also provides a new type of 3D porous materials for oil/water separation.

Acknowledgements

This work was financially supported by the National Natural Science Foundation of China (Nos. 51872210 and 51672194), the Program for Innovative Teams of Outstanding Young and Middle-aged Researchers in the Higher Education Institutions of Hubei Province, China (No. T201602), and the Key Program of Natural Science Foundation of Hubei Province, China (No. 2017CFA004).

Conflict of Interest

The authors declare no potential conflict of interest.

References

- [1] H.T. Zhu, S.S. Qiu, W. Jiang, D.X. Wu, and C.Y. Zhang, Evaluation of electrospun polyvinyl chloride/polystyrene fibers as sorbent materials for oil spill cleanup, *Environ. Sci. Technol.*, 45(2011), No. 10, p. 4527.
- [2] Y.C. Cheng, X.F. Li, Q. Xu, O. Garcia-Pineda, O.B. Andersen, and W.G. Pichel, SAR observation and model tracking of an oil spill event in coastal waters, *Mar. Pollut. Bull.*, 62(2011), No. 2, p. 350.
- [3] S. Songsaeng, P. Thamyongkit, and S. Poompradub, Natural rubber/reduced-graphene oxide composite materials: Morphological and oil adsorption properties for treatment of oil spills, *J. Adv. Res.*, 20(2019), p. 79.
- [4] M. Busto, E.E. Tarifa, and C.R. Vera, Extraction/adsorption as applied to the dearomatization of white mineral oil, *Chem. Eng. Res. Des.*, 146(2019), p. 239.
- [5] L. van Gelderen and G. Jomaas, Experimental procedure for laboratory studies of *in situ* burning: Flammability and burning efficiency of crude oil, *J. Vis. Exp.*, 135(2018), .
- [6] H.J. Chieng and M.F. Chong, Boron adsorption on palm oil mill boiler (POMB) ash impregnated with chemical compounds, *Ind. Eng. Chem. Res.*, 52(2013), No. 41, p. 14658.
- [7] V.M.F. Alexandre, F.V. do Nascimento, and M.C. Cammarota, Ammonia stripping, activated carbon adsorption and anaerobic biological oxidation as process combination for the treatment of oil shale wastewater, *Environ. Technol.*, 37(2016), No. 20, p. 2608.
- [8] S. Ullah, S. Hussain, W. Ahmad, H. Khan, K.I. Khan, S.U. Khan, and S. Khan, Desulfurization of model oil through adsorption over activated charcoal and bentonite clay composites, *Chem. Eng. Technol.*, 43(2020), No. 3, p. 564.
- [9] L. Zhang, H.Q. Li, X.J. Lai, X.J. Su, T. Liang, and X.R. Zeng, Thiolated graphene-based superhydrophobic sponges for oil-water separation, *Chem. Eng. J.*, 316(2017), p. 736.
- [10] Q. Zhu, Q.M. Pan, and F.T. Liu, Facile removal and collection of oils from water surfaces through superhydrophobic and superoleophilic sponges, *J. Phys. Chem. C*, 115(2011), No. 35, p. 17464.
- [11] N. Jiang, R. Shang, S.G.J. Heijman, and L.C. Rietveld, Adsorption of triclosan, trichlorophenol and phenol by high-silica zeolites: Adsorption efficiencies and mechanisms, *Sep. Purif. Technol.*, 235(2020), art. No. 116152.
- [12] R.P. Li, C.Y. Lin, and X.T. Liu, Adsorption of tungstate on kaolinite: Adsorption models and kinetics, *RSC Adv.*, 6(2016), No. 24, p. 19872.
- [13] Y. Zhao, F. Liu, and X.P. Qin, Adsorption of diclofenac onto goethite: Adsorption kinetics and effects of pH, *Chemosphere*, 180(2017), p. 373.
- [14] S. Ahmed, A. Ramli, S. Yusup, and M. Farooq, Adsorption behavior of tetraethylenepentamine-functionalized Si-MCM-41 for CO₂ adsorption, *Chem. Eng. Res. Des.*, 122(2017), p. 33.
- [15] H.Y. Wang, E.Q. Wang, Z.J. Liu, D. Gao, R.X. Yuan, L.Y. Sun, and Y.J. Zhu, A novel carbon nanotubes reinforced superhydrophobic and superoleophilic polyurethane sponge for selective oil-water separation through a chemical fabrication, *J. Mater. Chem. A*, 3(2015), No. 1, p. 266.
- [16] D. Tian, R.Y. Chen, J. Xu, Y.W. Li, and X.H. Bu, A three-dimensional metal-organic framework for selective sensing of nitroaromatic compounds, *APL Mater.*, 2(2014), No. 12, art. No. 124111.
- [17] J.T. Wang and Y.A. Zheng, Oil/water mixtures and emulsions separation of stearic acid-functionalized sponge fabricated via a facile one-step coating method, *Sep. Purif. Technol.*, 181(2017), p. 183.
- [18] X.M. Chen, J.A. Weibel, and S.V. Garimella, Continuous oil-water separation using polydimethylsiloxane-functionalized melamine sponge, *Ind. Eng. Chem. Res.*, 55(2016), No. 12, p. 3596.
- [19] A.A. Nikkhah, H. Zilouei, A. Asadinezhad, and A. Keshavarz, Removal of oil from water using polyurethane foam modified with nanoclay, *Chem. Eng. J.*, 262(2015), p. 278.
- [20] E.V. Gorb, P. Hofmann, A.E. Filippov, and S.N. Gorb, Oil adsorption ability of three-dimensional epicuticular wax coverages in plants, *Sci. Rep.*, 7(2017), No. 1, art. No. 45483.
- [21] Y. Feng and J.F. Yao, Design of melamine sponge-based three-dimensional porous materials toward applications, *Ind. Eng. Chem. Res.*, 57(2018), No. 22, p. 7322.
- [22] Q.H. Wang, Y.W. Li, S.L. Jin, S.B. Sang, Y.B. Xu, X.F. Xu, and G.H. Wang, Enhanced mechanical properties of Al₂O₃-C refractories with silicon hybridized expanded graphite, *Mater. Sci. Eng. A*, 709(2018), p. 160.
- [23] Q. Gu, T. Ma, F. Zhao, Q.L. Jia, X.H. Liu, G.Q. Liu, and H.X. Li, Enhancement of the thermal shock resistance of MgO-C slide plate materials with the addition of nano-ZrO₂ modified magnesium aggregates, *J. Alloys Compd.*, 847(2020), art. No. 156339.
- [24] D.H. Ding, L. Lv, G.Q. Xiao, J.Y. Luo, C.K. Lei, Y. Ren, S.L. Yang, P. Yang, and X. Hou, Improved properties of low-carbon MgO-C refractories with the addition of multilayer graphene/MgAl₂O₄ composite powders, *Int. J. Appl. Ceram. Technol.*, 17(2020), No. 2, p. 645.
- [25] M.Q. Liu, J.T. Huang, Q.M. Xiong, S.Q. Wang, Z. Chen, X.B. Li, Q.W. Liu, and S.W. Zhang, Micro-nano carbon structures with platelet, glassy and tube-like morphologies, *Nanomaterials*, 9(2019), No. 9, art. No. 1242.
- [26] X. Wang, Y. Chen, C. Yu, J. Ding, D. Guo, C.J. Deng, and H.X. Zhu, Preparation and application of ZrC-coated flake graphite for Al₂O₃-C refractories, *J. Alloys Compd.*, 788(2019), p. 739.
- [27] Q. Gu, F. Zhao, X.H. Liu, and Q.L. Jia, Preparation and thermal shock behavior of nanoscale MgAl₂O₄ spinel-toughened MgO-based refractory aggregates, *Ceram. Int.*, 45(2019), No. 9, p. 12093.
- [28] M.F. Elkady, Equilibrium and kinetics behavior of oil spill process onto synthesized nano-activated carbon, *Am. J. Appl. Chem.*, 3(2015), No. 3, art. No. 22.
- [29] T. Yao, Y.G. Zhang, Y.P. Xiao, P.C. Zhao, L. Guo, H.W. Yang, and F.B. Li, The effect of environmental factors on the adsorption of lubricating oil onto expanded graphite, *J. Mol. Liq.*, 218(2016), p. 611.

- [30] M. Wiśniewski, P.A. Gauden, A.P. Terzyk, P. Kowalczyk, A. Pacholczyk, and S. Furmaniak, Detecting adsorption space in carbon nanotubes by benzene uptake, *J. Colloid Interface Sci.*, 391(2013), p. 74.
- [31] S.S. Li, J.H. Liu, J.K. Wang, L. Han, H.J. Zhang, and S.W. Zhang, Catalytic preparation of graphitic carbon spheres for Al_2O_3 -SiC-C castables, *Ceram. Int.*, 44(2018), No. 11, p. 12940.
- [32] S.S. Li, J.H. Liu, J.K. Wang, Q. Zhu, X.W. Zhao, H.J. Zhang, and S.W. Zhang, Fabrication of graphitic carbon spheres and their application in Al_2O_3 -SiC-C refractory castables, *Int. J. Appl. Ceram. Technol.*, 15(2018), No. 5, p. 1166.
- [33] S.S. Li, F.L. Li, J.K. Wang, L. Tian, H.J. Zhang, and S.W. Zhang, Preparation of hierarchically porous graphitic carbon spheres and their applications in supercapacitors and dye adsorption, *Nanomaterials*, 8(2018), No. 8, art. No. 625.
- [34] A. Kozbial, C. Trouba, H.T. Liu, and L. Li, Characterization of the intrinsic water wettability of graphite using contact angle measurements: Effect of defects on static and dynamic contact angles, *Langmuir*, 33(2017), No. 4, p. 959.